IOP Publishing Measurement Science and Technology
Meas. Sci. Technol. 31 (2020) 045202 (15pp) https://doi.org/10.1088/1361-6501/ab491b

Ultrasonic measurement of air temperature along the axis of a laser beam during interferometric measurement of length

Marek Dobosz and Marek Ściuba

Warsaw University of Technology, Faculty of Mechatronics, Institute of Metrology and Biomedical Engineering, Św. A. Boboli 8 st., 02-525 Warszawa, Poland

E-mail: dobosz@mchtr.pw.edu.pl

Received 15 June 2019, revised 9 September 2019
Accepted for publication 30 September 2019
Published 9 January 2020

Abstract

An ultrasonic technique that allows compensation of air temperature changes and gradients along the beam axis of the laser interferometer during displacement measurement is presented.

The system is based on using two ultrasonic paths parallel to the laser beam that operate at different frequencies and continuous waves emitted in opposite directions. The theoretical basis of the measurements is presented. To enable ultrasonic temperature measurement when the measuring reflector is moving, an iterative measurement algorithm is proposed. Experimental assessment of the accuracy of the method is presented. The effect of air temperature gradients along the laser beam axis is tested. The influence of air flow on the measurement accuracy is analyzed.

Keywords: interferometer distance measurement, Edlén's formula, temperature compensation in interferometer length measurement, ultrasonic temperature measurement

(Some figures may appear in colour only in the online journal)

1. Introduction

In interferometric length measurements the wavelength of the light usually acts as a length master. Determining the wavelength of light based on the frequency of the electromagnetic wave emitted by the laser requires knowledge of the refractive index of the environment in which the beam propagates. Interferometric methods of dimensional measurements are easily suited to laboratory conditions in which high stability of ambient conditions is ensured, guaranteeing accurate determination of the refractive index of the air, and thus of the wavelength of light.

Growing expectations regarding the accuracy of measurements mean that these methods are adapted for use in industrial conditions, where the spatial and temporal variability of environmental conditions is many times greater than in laboratory conditions. One of the main problems to be solved is the minimization of the measurement error caused by the influence of the aforementioned variability of the ambient conditions.

There have been attempts to introduce ultrasonic measurements to correct the impact of changes in the refractive index in displacement measurements [1–6]. The research studies presented in the above-mentioned publications were performed for distances ranging from 2 to 30 m and with measurement uncertainties from 0.01 °C to 0.1° C. Several techniques of ultrasonic temperature measurement that can also be applied in distance measuring interferometers are described in publications (e.g. [7–12]). The measuring systems used in these studies can be divided into the following three groups: (i) depending on the direction of ultrasonic measurement: unidirectional [1, 2, 7, 10–12], bidirectional monorail [3, 6, 8, 9] and bidirectional two-way measurements [4, 5]; (ii) depending on the generation technique of the ultrasonic wave: with a continuous wave and measurement of the phase of the signal [1, 10] and with the generation of a packet of pulses [4, 5, 8, 9, 11]; and (iii) depending on the change in the measuring distance: with a fixed [7–9, 11, 12] and variable [2–6, 10] measuring distance.

The unidirectional measurement [1, 2, 7, 10–12] (figure 1(a)) takes place in a single ultrasonic measurement path. This track

is placed parallel to the interference measurement axis, a short distance from it. This distance depends on the design of the receiver, and for an uncompressed transducer it ranges from 30 to 40 mm. When using a mirror that focuses ultrasonic waves (figure 1(b)), the distance is greater and may reach 27 m [2].

Applying the ultrasonic mirror [6] is necessary for measurements of large distances (above a few meters), because the signal reaching the receiver is weakened. The unidirectional method is only suitable for measurements during which no disturbing air flow occurs. Synchronization between the transmitter and receiver is necessary. It is carried out by two pulses: starting at the moment of sending the ultrasonic pulse, and stopping at the time of receiving this pulse. Depending on the design of the measuring set-up, the start pulse can be sent via a cable or wirelessly, e.g. optically (light flash). Wireless transmission is more advantageous for distances in the measurement path greater than a few meters.

In bidirectional two-way measurement [4, 5] (figure 1(c)) two ultrasound tracks are placed on two sides of the interference path, at the same distance from it. Measurements in opposite directions for tracks operating on the same frequency are made alternately, but for tracks operating at different frequencies they are made simultaneously. The result of the measurement is the value averaged from readings in opposite directions. The doubling of ultrasound tracks minimizes the influence of the distance between ultrasonic and interference paths. Bidirectional measurement provides partial compensation of the laminar air flow along the measuring path.

Another type of ultrasonic measurement is shown in figure 1(d) [6, 8, 9]. It is a measuring system with one ultrasonic path, with a single transceiver unit and an ultrasonic reflector. The ultrasonic signal emitted from the transmitter goes to the reflector, where it is reflected. The return signal is received by the receiver. It can be the same piezoelectric element that is used when transmitting, or the second one next to it. The measuring cycle consists of the emission of a pulse pack, damping the transmitter, switching to receive and receive the signal. Due to the time needed to change the direction of transmission, the minimum distance should be greater than 100 mm.

When measuring with a continuous wave in unidirectional measurement, (according to figure 1(a)) the phase between the transmitted and received signal is measured and converted into the speed of sound. The emitted signal acts as a reference, and the signal received is the measuring signal. With the 10 ns uncertainty of measuring the time between the edges of transmitted and received signals, assuming that the measuring distance is equal to e.g. 1 m, and the speed of sound is 350 m s^{-1} (for 25 °C) we can easily calculate the measurement time equal to 2.86 m s^{-1}. It gives the relative uncertainty of determining the speed of sound equal to $3.5 \cdot 10^{-6}$ at ameasuring distance of 1 m. The condition for obtaining such metrological parameters is the generation of enough narrow signal beam from the emitter and the attenuation of reflection near the receiver. The beam cannot be obscured during the displacement because it causes loss of position information. When measuring with a continuous wave it is also necessary to provide a measurement of the distance of the transmitter and receiver in order to determine the speed of sound. The ultrasonic wave travel time is determined by counting the transitions of the signal phase changes by the zero level.

When measuring with a pulse pack, the problem is to clearly determine the beginning of the received pack. For this purpose, various techniques are used. The simplest method [13, 14] consists of determining the threshold level of the signal from the detector, beyond which the time counter is stopped. This method is effective if the measurements are carried out at a constant distance. The level of the received signal decreases in the square of the distance [15]. As a result of this suppression, the detection of the package occurs with a delay corresponding to the duration of the pulses with an amplitude smaller than the registration threshold. As the distance increases, the error will increase as the amplitude of the signal falls. A more accurate future alternative for detecting the beginning of an ultrasonic wave packet is the Akaike information criterion (AIC) (e.g. [16, 17]).

To improve the range and unambiguous identification of the received pulse, various types of modulation of the transmitted signal are used. The initial signal stimulates the vibrations in the receiver, and the introduced disturbance enables an easy to detect signal change. It may be a phase modulation [11, 12, 18], where a step change in the phase of the transmitted signal and a temporary attenuation of the received signal take place. The time between the phase change in the emitted signal and the pulses received after a short loss of signal from the detector is measured. This technique requires the use of ultrasonic elements with a low inertia and a wide band of the received signal—so that the received signal has attenuated an as short as possible fragment of the transmitted signal. However, such devices have a lower sensitivity, which reduces the distance at which they can work properly.

Another way to identify the pulse received in the ultrasound path is to change the frequency of the transmitted signal [10, 19]. Ultrasound elements operating with a wide signal frequency band are required for a system with a frequency change. If the change of frequency emitted in the measurement path is large, it will be easily detected, but most often it will cause the path to operate outside the central frequency, i.e. the resonance frequency of the transmitter and receiver. With this work, the signal is strongly suppressed, and thus the effective measuring range is reduced. If the frequency changes are small, the track sensitivity will be maintained, but there may be a problem with the precise detection of the moment of frequency change.

Most of the tests reported in the literature were performed on a fixed measurement distance [7–9, 11, 12, 18, 20]. Only a few studies [2–6, 10] were carried out on a variable distance. Additionally, even then the displacement measured by the interferometer did not exceed 1 m at the measuring distance of 5 m (i.e. the ultrasonic measurement was possible from 4 to 5 m distance).

The article presents the theoretical basis and the technical solution, as well as the experimental results of the ultrasonic technique that allow compensation of air temperature changes and gradients along the beam axis of the laser interferometer

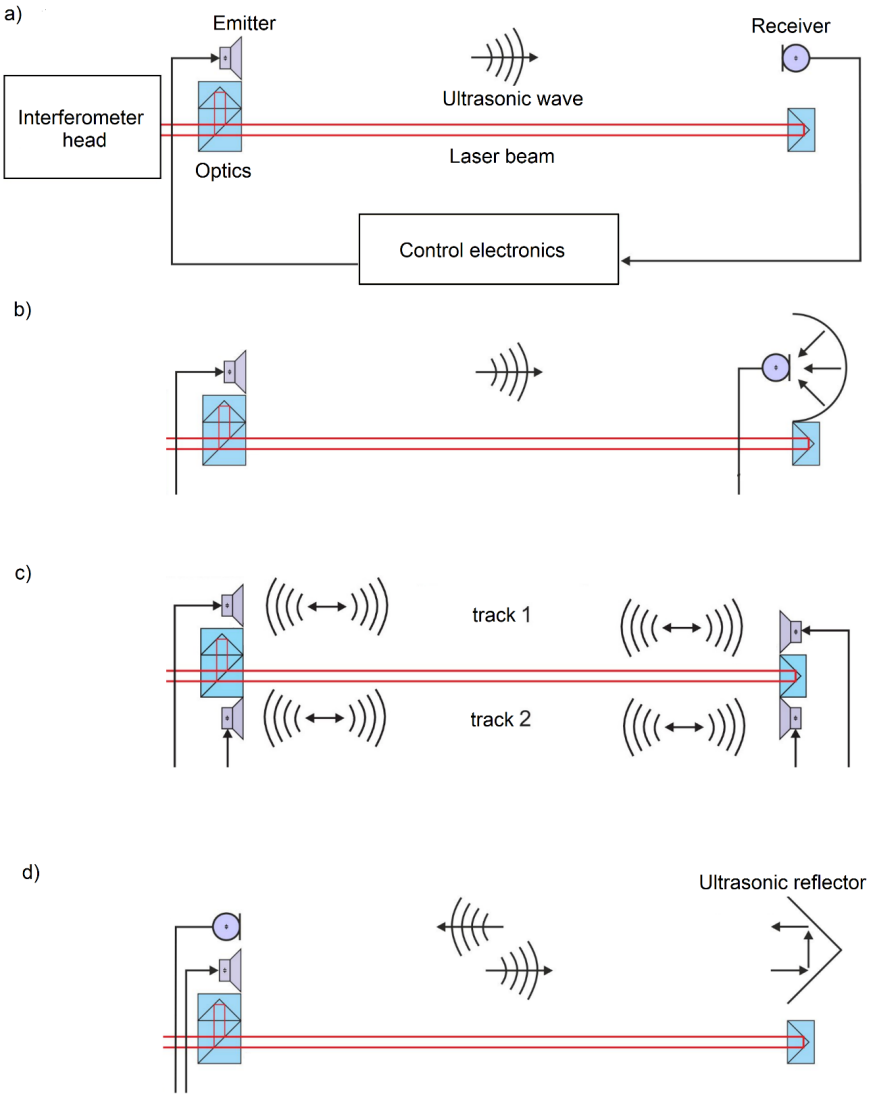

Figure 1. Techniques of ultrasonic temperature measurement along the axis of the interferometer laser beam. (a) Unidirectional measurement, (b) unidirectional measurement with a mirror that focuses ultrasonic waves, (c) bidirectional measurement with two ultrasound tracks, (d) bidirectional measurement with an ultrasonic reflector.

during the displacement measurement. The proposed technique is insensitive to air flow and usable at variable measuring distances.

2. Theoretical basis

2.1. Relationship between sound propagation speed and air temperature

According to the Newton–Laplace equation the speed of sound ν in an ideal gas is given by the equation (e.g. [21]):

$$\nu = \sqrt{\frac{\chi \cdot p}{\rho}} \tag{1}$$

where χ is the adiabatic constant (also referred to as the adiabatic exponent, the specific heat ratio or the isentropic exponent), p is the absolute pressure of the gas and ρ is the density of the gas. If the analyzed gas is moist air, the adiabatic exponent depends mainly on the partial pressure of the water vapor p_w and air pressure p, and may be evaluated from the dependence [21–23]:

$$\chi = 1.41\frac{p - p_w}{p} + 1.33\frac{p_w}{p} = 1.41 - 0.08\frac{p_w}{p} \tag{2}$$

where p_w represents the mole fraction (or partial pressure) of water vapor [23]. The coefficient 1.41 in the above equation represents the specific heat capacity ratio of the mixture: dry air (with the adiabatic constant 1.4) with 1% of argon (with the specific heat capacity ratio 1.67) [24]. The value 1.33 refers to the specific heat capacity ratio of water vapor (e.g. [25]). The partial pressure of water vapor p_w (in pascals) is calculated from the relative humidity according to the equation:

$$p_w = p_v\frac{H_R}{100} \tag{3}$$

where p_v is the water vapor partial pressure (saturated vapor pressure over water) in pascals. Here, H_R is the relative humidity in percent (ranging numerically from 0 to 100).

To take into account air humidity together with temperature a water vapor partial pressure (saturated vapor pressure over water), p_v (in pascals), is approximated by the Tetens equation [26, 27]:

$$p_v = 610.8 \cdot e^{\frac{17.269t}{237.3+t}} \tag{4}$$

where the temperature t is in degrees Celsius (°C). The density of air ρ can be evaluated from [21]:

$$\rho = \frac{pM}{RT} \tag{5}$$

where p is the air pressure in pascals, M is the average molar mass (in grams per mole) and $T$is the absolute temperature. Here, R is the ideal, or universal, gas constant, with the value of $R = 8.314\,459\,848$ J $(\mathrm{K} \cdot \mathrm{mol})^{-1}$. According to Dalton's law, the air pressure p is calculated as the sum of the partial pressures, i.e.:

$$p = p_d + p_w \tag{6}$$

where p_d and p_w represent the partial pressures of dry air and water vapor, respectively.

The average molar mass M is equal to the sum of the mole fractions of each gas multiplied by the molar masses of that particular gas [23]:

$$M = \frac{p_d}{p}M_d + \frac{p_w}{p}M_w \tag{7}$$

where M_d is a molar mass of dry air, and M_w is a molar mass of water vapor. By substituting equations (6) and (7) into (5), we obtain the formula for the air density in the form:

$$\rho = \frac{pM_d - p_w(M_d - M_w)}{RT}. \tag{8}$$

The density of humid air may be calculated by treating it as a mixture of ideal gases. In this case, the partial pressure of water vapor is known as the vapor pressure. Using this method, the error in the density calculation is less than 0.2% in the range of −10 °C to 50 °C.

Finally, after substituting equations (2) and (8) into (1), and after performing the necessary transformations, the absolute temperature of the medium can be determined as a function of the sound wave speed propagation in this medium according to the relationship:

$$T = \nu^2 \frac{pM_d - p_w(M_d - M_w)}{R(1.41p - 0.08p_w)} = \nu^2 Q. \tag{9}$$

The quotient appearing in this formula is denoted by the parameter Q. The above relationship shows that the absolute temperature T of the measured air is a quadratic function of the velocity ν of the sound propagation. It also depends on the air pressure p and the content of water vapor in it (strictly the partial pressure p_w of water vapor). The temperature T is expressed in kelvins. The temperature in °C is calculated from the following dependence:

$$t = T - 273.15. \tag{10}$$

The velocity ν of sound propagation in the air can be measured by the time t_m of the fly over the length Δl of the measurement distance:

$$\nu = \frac{\Delta l}{t_m}. \tag{11}$$

The length Δl is obtained from the initial reading of the interferometer.

If temperature gradients appear along the measurement length an average value $\bar{\nu}$ obtained from the velocity distribution $\nu(l)$ along the measurement length can be treated as the ultrasonic wave velocity, i.e.:

$$\bar{\nu} = \frac{1}{\Delta l}\int_0^{\Delta l} \nu(l)\,\mathrm{d}l. \tag{12}$$

2.2. Determination of the displacement by the interferometer

In interferometric length measurements, the measurement is based on determining the change in the fringe phase $\Delta\varphi_I$ caused by the displacement of the reflector. This phase change is determined by the so-called counting fringe method. The result of the interferometric measurement is obtained from the dependence [28]:

$$\Delta\varphi_I = \frac{4\pi n\Delta l}{\lambda} \tag{13}$$

where n is the refractive index of the medium, λ is the wavelength in vacuum and Δl represents the measured displacement. The uncertainty of the wavelength determination is the basic source of the uncertainty in interference measurements of length.

The wavelength's instability in the vacuum of lasers used in metrology does not exceed 10^{-9} h^{-1}, and it is negligible in comparison with the instability of the wavelength in air.

If the refractive index of the medium along the measuring axis is variable then the total phase change $\Delta\varphi_I$ in the interferometer can be calculated as the sum of the partial phase changes $\delta\varphi_i$ (from $i = 1$ to k) on any short measurement sections of the same length δl:

$$\Delta\varphi_I = \delta\varphi_1 + \delta\varphi_2 + \ldots \delta\varphi_k = \frac{4\pi\delta l}{\lambda}$$
$$(n_1 + n_2 + \ldots n_k) = \frac{4\pi k\delta l}{\lambda k}\sum_{i=1}^{k} n_i = \frac{4\pi\Delta l}{\lambda}\bar{n} \tag{14a}$$

where $\bar{n}$ represents the average value of the refractive index over the entire measuring path Δl and can also be expressed as:

$$\bar{n} = \frac{1}{\Delta l}\int_0^{\Delta l} n\mathrm{d}l. \tag{14b}$$

Currently, in metrological practice there are two methods used for determining the refractive index of air: (i) the modified Edlén technique [29–31] used for wavelengths around 633 nm, and (ii) the Ciddor equation [32, 33], applicable to

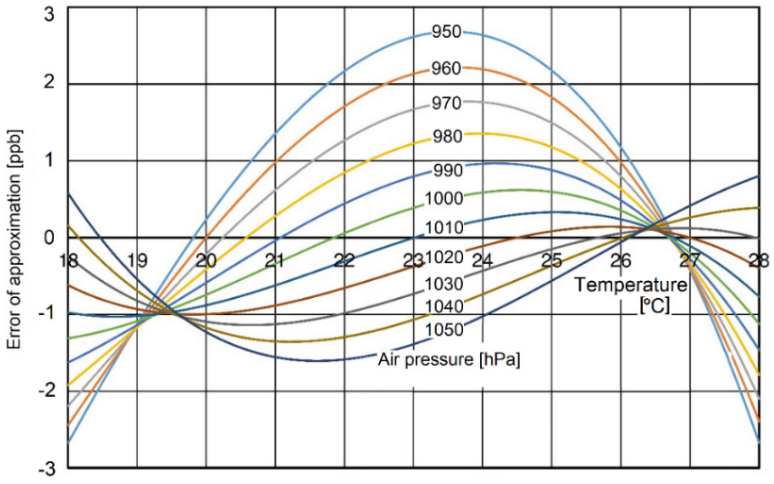

Figure 2. An illustration of the obtained approximation error.

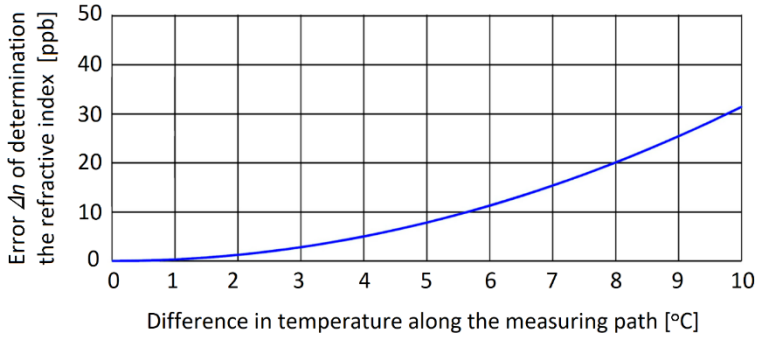

Figure 3. The error Δn of determination of the refractive index as a function of the temperature difference for the case of its linear change in the measurement path.

any wavelength of light. The refractive index calculated by the Edlén formula is the sum of the coefficient for the wavelength of light in the vacuum and corrections resulting from temperature, pressure and humidity.

According to Edlén's formula, standard air (i.e. dry air at 1 atmosphere, 15 °C, containing 300 ppm by volume of CO_2) has a refractive index of air n_s equal to:

$$n_s = 1 + 10^{-8} \cdot \left(8342.54 + \frac{2406\ 147}{130 - \frac{1}{\lambda^2}} + \frac{15\ 998}{38.9 - \frac{1}{\lambda^2}} \right) \quad (15)$$

where λ is the laser vacuum wavelength expressed in micrometers.

The refractive index n_{tp} of air under the conditions of temperature t (in °C), air pressure p (in pascals), is equal to:

$$n_{tp} = 1 + (n_s - 1)\frac{p}{96\ 095.43} \cdot \left[\frac{1 + 10^{-8} \cdot (0.601 - 0.009\ 72 \cdot t) \cdot p}{1 + 0.003\ 661 \cdot t} \right]. \quad (16)$$

To take into account the air humidity based on equations (3) and (4) the following amendment for the refractive index is determined:

$$n_w = 10^{-10} \cdot \frac{292.75}{273.15 + t} \left(3.7345 - \frac{0.0401}{\lambda^2} \right) \cdot p_w. \quad (17)$$

Then, corrected for variation of the water vapor index of refraction, n_E can be written in the form:

$$n_E = n_{tp} - n_w. \quad (18)$$

2.3. The effect of temperature gradients on the ultrasonic measurement result

Edlén's formulas given above, due to the complexity of the form, makes it difficult to conduct further analysis. Therefore, we proposed to approximate this dependence in the considered conditions with the second-order polynomial, i.e.:

$$n = 1 + A + Bp + t\,(C + Dp) + t^2\,(E + Fp) + Gp_w \quad (19)$$

where $A, B, \ldots G$, are polynomial coefficients, t is the air temperature in °C, p and p_w are the air and water vapor pressures, respectively. The approximation was performed using the bisection method to obtain the smallest possible difference between the results obtained from Edlén's rule (formulas from (15) to (18)) and from the approximate formula (19). The approximation was made for the temperature range $t = 18$ °C $\div$ 28 °C, pressure $p = 950 \div 1050$ hPa and relative humidity RH $= 0\% \div 100\%$ (converted to water vapor pressure in accordance with equations (3) and (4)). The obtained following coefficients: $A = 1.385\ 15 \cdot 10^{-6}$; $B = 2.86 \cdot 10^{-9}$; $C = -1.3493 \cdot 10^{-7}$; $D = -9.0715 \cdot 10^{-12}$; $E = 3.001\ 23 \cdot 10^{-9}$; $F = 1 \cdot 10^{-15}$; $G = -3.634 \cdot 10^{-10}$ give the differences between formulas less than 2.75^{-9}.

A graph of the differences between Edlén's formulas and its approximation by equation (19) is shown in figure 2 [34].

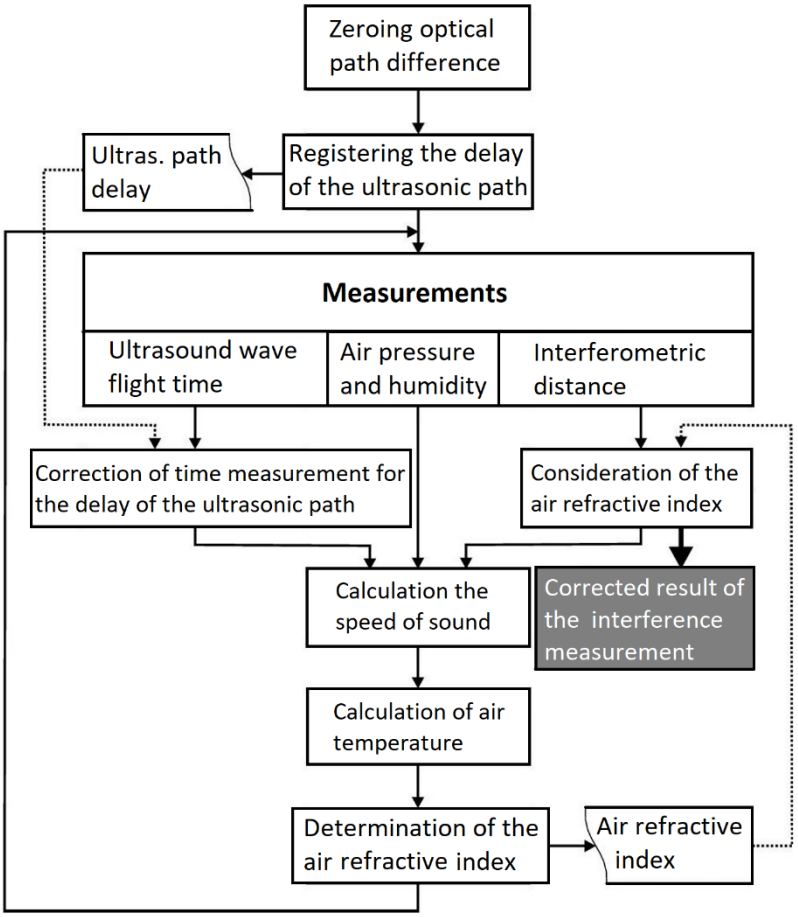

Figure 4. The measurement algorithm.

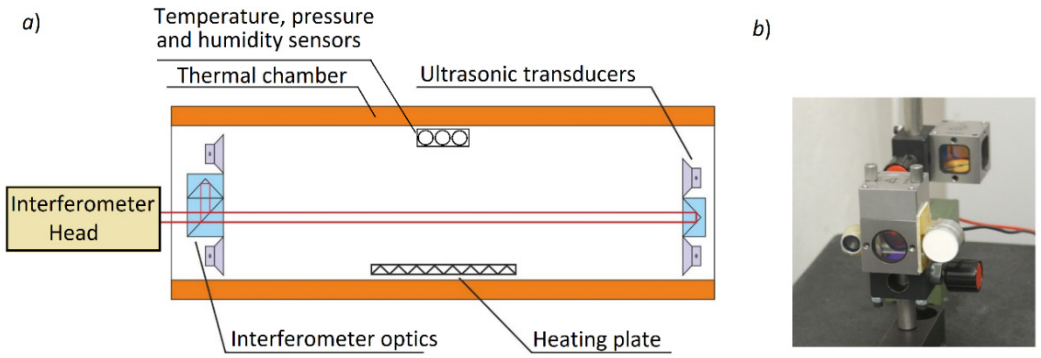

Figure 5. (a) The experimental set-up for testing the accuracy of the ultrasonic measurements. (b) Placing ultrasonic transducers on the optical elements of the interferometer (view after removing the tunnel).

The obtained level of approximation is satisfactory for further analysis.

The following parts of equation (19) are constant during the measurement and do not depend on the temperature

$$\begin{aligned} M &= C + D \cdot p \\ N &= E + F \cdot p \\ O &= A + B \cdot p + G \cdot p_{\mathrm{w}}. \end{aligned} \tag{20}$$

The values of these coefficients calculated for normal conditions ($t = 20\ ^{\circ}\mathrm{C}$, $p = 1013.25$ hPa, $p_{\mathrm{w}} = 1.333$ Pa) are equal: $M = -2.741\ 392 \cdot 10^{-6}$; $N = 3.089\ 75 \cdot 10^{-9}$; $O = 8.1038 \cdot 10^{-4}$. By also assuming the molar mass of dry air $M_{\mathrm{d}} = 28.979\ \mathrm{g\ mol^{-1}}$, and the molar mass of water vapor $M_{\mathrm{w}} = 18\ \mathrm{g\ mol^{-1}}$ we obtain, for normal conditions, the value of parameter Q in equation (9) equal to 20.156 157.

Knowing the values of the above-mentioned parameters, we can express the average refractive index along the measuring distance in the following form:

$$\bar{n} = \frac{1}{\Delta l} \int_0^{\Delta l} \left[1 + O + M\left(Q\nu(l)^2 - 273\right) + N\left(Q\nu(l)^2 - 273\right)^2\right] \mathrm{d}l \tag{21}$$

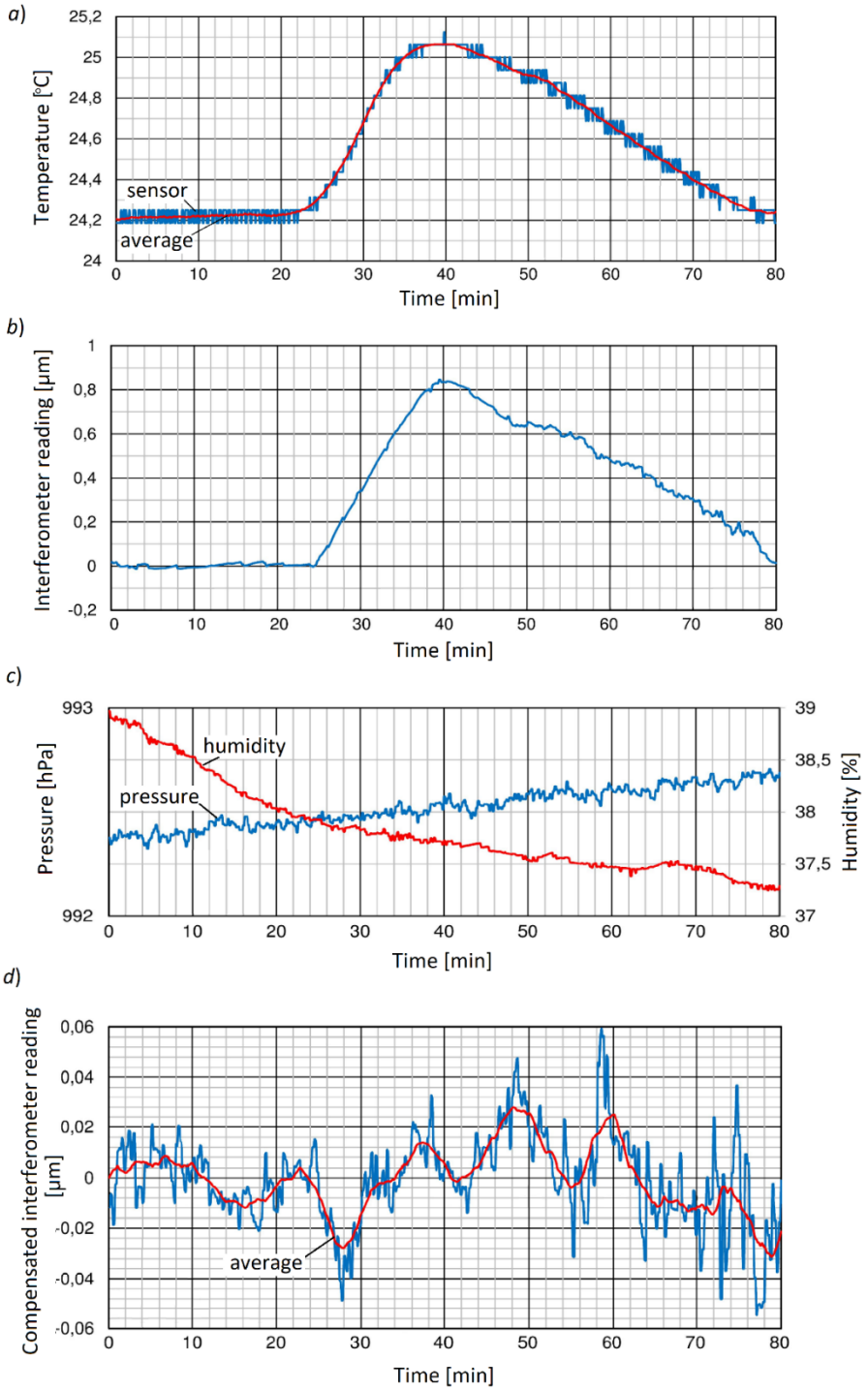

Figure 6. Sample results from testing the accuracy of the temperature measurement using the ultrasound technique. (a) Generated changes in air temperature, (b) observed changes in the interferometer readings without compensation of ambient conditions, (c) changes in the air pressure and humidity during the experiment, and (d) compensated interferometer readings based on ultrasonic temperature measurement.

where Q is defined by equation (9). This is the air refractive index calculated on the basis of the average value obtained from the instantaneous sound velocities. Unfortunately, without knowing the temperature distribution, and thus the distribution of the speed of sound propagation along the measuring path, we cannot use the given relationship in practice.

Measuring the average velocity of sound propagation along the measurement path according to the dependence (11), and taking into consideration the dependence (14*b*) de facto we use the equation:

$$\bar{n}_U = 1 + O + M\left(\frac{Q}{\Delta l}\int_0^{\Delta l}\nu(l)^2\mathrm{d}l - 273\right) + N\left(\frac{Q}{\Delta l}\int_0^{\Delta l}\nu(l)^2\mathrm{d}l - 273\right)^2. \tag{22}$$

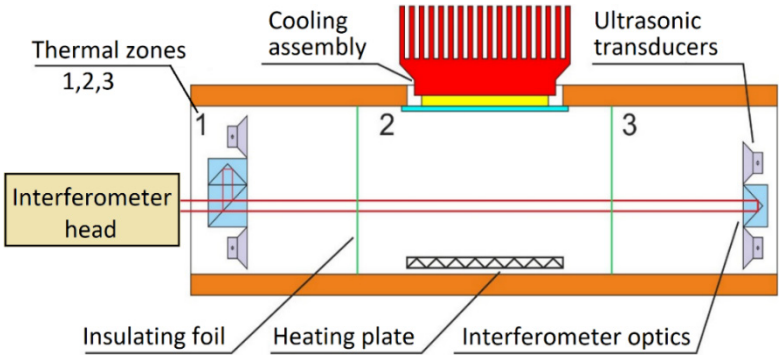

Figure 7. The experimental set-up for testing the possibility of temperature gradient compensation using the ultrasonic technique.

A question arises as to the size of the measurement error that may occur when replacing the dependence (21) with equation (22). We will write this error as:

$$\Delta n = \bar{n} - \bar{n}_U. \tag{23}$$

To assess the permissible value of this error, let us assume the value of the maximum temperature gradient that can appear along the measurement path equal to, e.g. 0.1 °C/10 mm. Let us approximate the function of the temperature distribution along the measurement path by assembling it with 10 mm sections (δl) in the area in which the temperature increase is linear and does not exceed the assumed temperature gradient. It is easy to notice that the most disadvantageous case will occur when the maximum accepted gradient with the same sign appears simultaneously in all sections δl. Then, e.g. for $\Delta l = 1$ m, we will observe a temperature change of 10 °C. Values of the calculated error Δn for the temperature changes from 0 °C to 10 °C are shown in figure 3 [34].

Summing up, it can be concluded that the ultrasonic temperature measurement with negligible error takes into account an unknown temperature distribution occurring along the measurement path of the interferometer, which is impossible to achieve, even by measuring with multiple thermometers.

All the values determined in this way are much more advantageous than those obtained with the use of thermometers used in compensators of the ambient conditions in interferometers for displacement measurement.

2.4. Measuring algorithm

To enable ultrasonic temperature measurement with a moving measuring reflector, the algorithm for the measurement procedure is presented in figure 4. The first calibration measurement is performed for the approximately zero distance between the ultrasonic transmitter and the receiver and the zero optical difference of the interferometer (the interferometer's optical elements are then in contact). As a result of this measurement, information about the delay brought by the ultrasonic path is obtained. This value is subtracted from the time measurement result in subsequent measurements.

Because this measurement is performed for an approximately zero optical path difference, the lack of temperature correction does not cause a significant error. In the case of interferometric measurement this is due to the fact that by assuming a range of temperature changes in the laboratory of 23 °C ± 5 °C, the measurement uncertainty is at the level of 10^{-5}. For a measured distance less than 100 mm, the uncertainty of measurement is less than 1 μm. With ultrasonic measurement, with a time measurement resolution of 10 ns, such uncertainty in distance measurement does not affect the result of the velocity of the sound propagation. Next, the measured distance is increased. The interferometer and ultrasonic measurements are carried out continuously. In order to measure the speed of sound it is necessary to know the absolute distance between the transmitter and the receiver.

This distance is measured by the interferometer. The first reading of the interferometer is performed without thermal correction. But based on this reading the ultrasonic system determines the temperature. The value obtained in this way is next used to correct the indication of the interferometer. After this correction, the new value of the measured distance is entered into the ultrasound system, which again determines the temperature. This loop is performed in a continuous mode—each previous measurement corrects the next one. In practice, after several iterations, the obtained results become already accurate enough.

3. Experimental studies

A series of preliminary tests for ultrasonic temperature measurement led us to a solution in which two ultrasonic paths parallel to a laser beam operate at different frequencies and continuous waves are emitted in opposite directions. Such a configuration allowed us to apply the maximum of the measurement frequency equal to the frequency of ultrasonic waves used (measurements are performed in each period of the ultrasonic signal). These frequencies were equal to 40 kHz and 96 kHz. A short delay time (3 ms m^{-1}) provided a quick response to possible air movements in the measuring path. High frequency of measurements allows us to use the average of the results, e.g. when averaging over 2000 measurements, the frequency of the obtained results is greater than 20 Hz. In the experimental system we applied a set transmitter-receiver ITC-9071 (International Transducer Corp.) operating at a nominal frequency of 92 kHz, and a set MA40A5 (Jameco Electronics) for the frequency of 40 kHz.

The ultrasound wave flight time was determined based on the phase measurement between the transmitted and

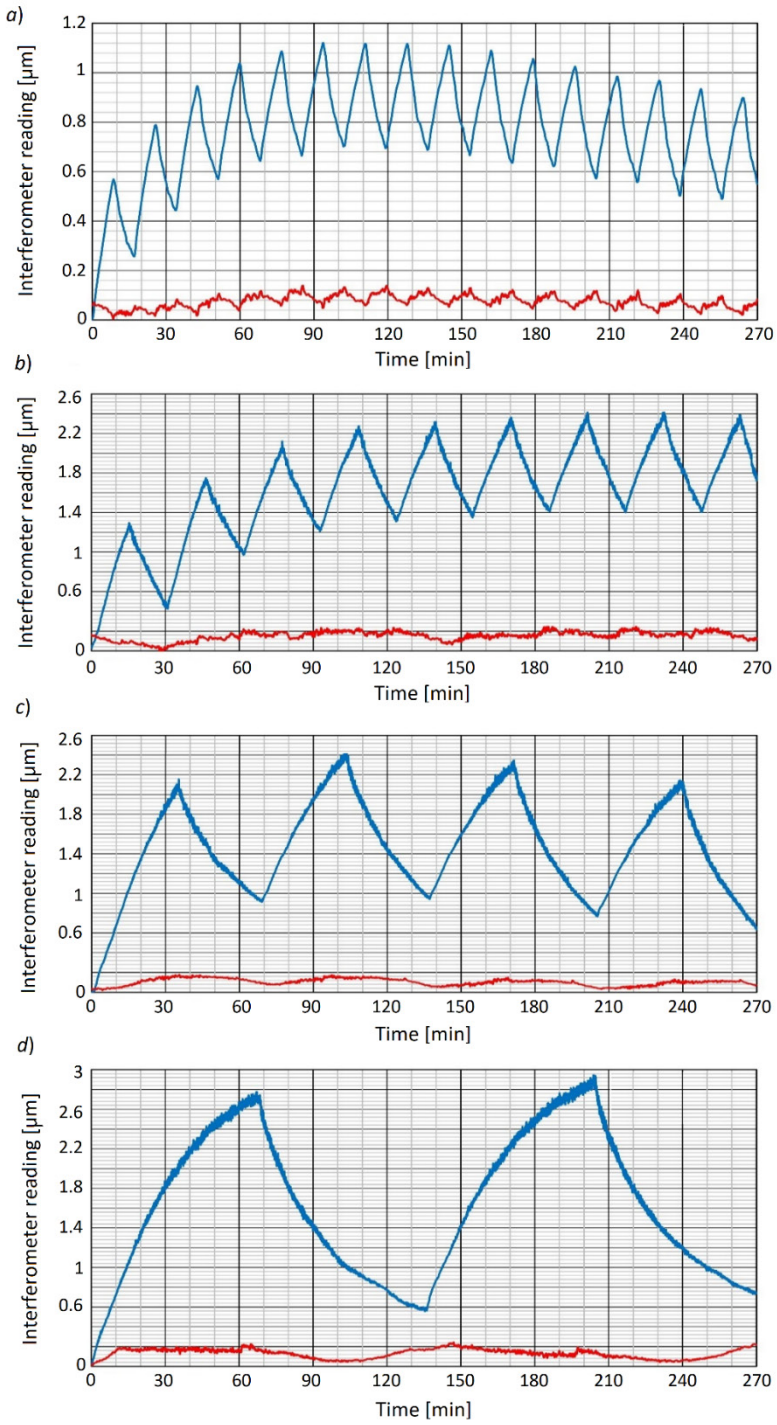

Figure 8. The results of tests of thermal compensation effectiveness using the ultrasonic method for cycles: (a) 16 min, (b) 32 min, (c) 64 min and (d) 130 min. The upper line in each graph shows the uncompensated results, and the bottom line refers to the results obtained after compensating the ambient conditions.

received signal rather than the basis of the direct time measurement. The phase shift in each period of the received signal was measured. If the phase shift between successive measurements was changed by more than 360 °, then the value of the period counter was changed. The ultrasonic wave travel time t_m was calculated from the following dependence:

$$t_m = t_s\left(z + \frac{\phi}{360^\circ}\right) \tag{24}$$

where t_s is the duration of one signal period of e.g. 24.4 µs for 40 KHz, z is the number of periods counted and ϕ is the measured phase shift. Then, using the formulas (9) and (10), the air temperature was calculated. Next, this value was used to calculate the refractive index based on equations (15)–(17).

3.1. Accuracy of ultrasonic temperature measurements

The accuracy of the ultrasonic temperature measurements was tested in the experimental set-up shown in figure 5.

The measuring paths of the interferometer and ultrasound system were fixed and placed in a temperature chamber to separate them from uncontrolled changes in ambient conditions. The components of the measuring system were located at a distance of 1 m from each other. To reduce the influence of temperature on the length of the measuring path, they were fixed outside the chamber to the bench. The ZLM 500 set (Zeiss) was used as the interferometer. A heating plate was placed in the middle of the track length to set the temperature changes. The plate temperature was changed cyclically, recording the results from the interferometer, ultrasound system, air pressure and humidity.

An electronic digital sensor type DS1631 (Maxim-Dallas) with a resolution of 0.0625 °C was used as a reference for temperature measurement. Its accuracy after precise calibration based on curve fitting to the data from the manufacturer's specification was equal to ±0.02 °C. Pressure was measured by a VTI SCP1000 D01 absolute digital pressure sensor with a resolution of 1.5 Pa and accuracy of ±50 Pa. For the purpose of humidity measurement, we used a Sensirion SHR-11 digital sensor with resolution of 0.03% and accuracy of ±3%.

The sample results are illustrated in figure 6. Figure 6(a) shows the generated temperature changes. As we can see in figure 6(a) the temperature variability reached 1 °C. The observed vertical lines show the sensor discretization error. The middle line represents the average value of the registered temperature. The graph in figure 6(b) shows the changes in the optical path difference indicated by the interferometer (the geometrical distance remains constant) during the temperature change. These changes are consistent with temperature changes (the correlation coefficient equals 0.98). The amplitude of this change is equal to 8.5 μm. This is an error of the thermally uncompensated interferometric length measurement (of the distance equal to 1 m when air temperature changes reach 1 °C). Figure 6(c) shows the pressure (increasing line) and humidity (falling line) changes observed during the test. These changes were, respectively, 0.4 hPa and 1.5% during the test. Finally, figure 6(d) shows the compensated results of the interference distance measurement taking into account the temperature measured by the ultrasound system and the pressure and humidity changes registered by the sensors (shown in figure 6(c)). The line with higher frequencies represents individual readings. The center line represents data averaged from 30 readings. The range of the averaged results is within ±0.03 μm. The observed variability of the results may be caused, among other things, by a small change in the geometric path in the interferometer emerging from the thermal expansion of the set-up base.

The range ±0.03 μm corresponds to a temperature change of approx. ±0.03°C. This inaccuracy is similar to that obtained with the spot thermometer. However, this inaccuracy concerns the value determined for the entire length of the measurement path, in real time. In the case of the point thermometer, this value only applies to the small sensor environment, and it is achieved with a long reaction time.

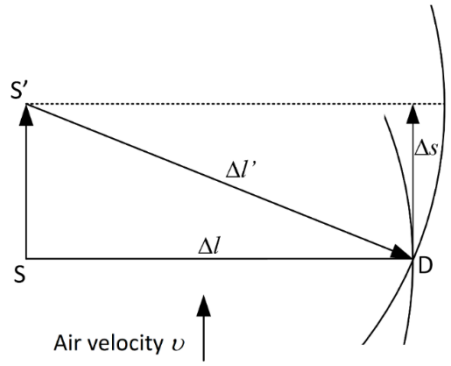

Figure 9. Shift of the ultrasound wavefront under the influence of the transverse air movement.

3.2. The effect of air temperature gradients along the laser beam axis

To test the effect of air temperature gradients along the laser beam axis the experimental set-up was modified according to the diagram shown in figure 7.

To accelerate the temperature changes, in addition to the heating module, an additional cooling module was introduced. Above the heating element in the central part of the chamber we placed a cooling (Peltier) module. These elements worked alternately, providing cyclic temperature changes in the middle part of the measuring chamber. With the help of isolation foil, the chamber was divided into three zones according to the drawing. Additionally, inside the chamber there was a sensor module registering changes in temperature, humidity and atmospheric pressure. The temperature outside the chamber was also measured. The entire set-up was placed on a table made of granite slab, thermally insulated from the environment. Measurements were carried out in series lasting 6–7 h. During this time, heating–cooling cycles were generated, with a duration of 15–140 min depending on the measurement series. This method of thermal influence was used to keep the average temperature as constant as possible in the chamber. The laser interferometer wavelength correction during its operation was turned off. After completing the measurement series, all the results were analyzed off-line, including the calculation of the wavelength correction.

Sample results from the experiment are shown in figure 8. All the graphs show changes in the interferometer readings during the tests (top lines) and after the correction of wavelength based on the pressure and humidity sensor indications as well as ultrasonic temperature measurement (bottom lines). The observed change in the readings of the interferometer after the temperature correction based on ultrasonic measurement decreases approximately five times. For short-term changes (16 min cycle—figure 8(a)), incomplete compensation of temperature changes was observed. The influence of uneven signal delays from interference and ultrasonic measurement probably resulted from the method used to average the results. However, the variability in the results of the interference measurements resulting from thermal gradients

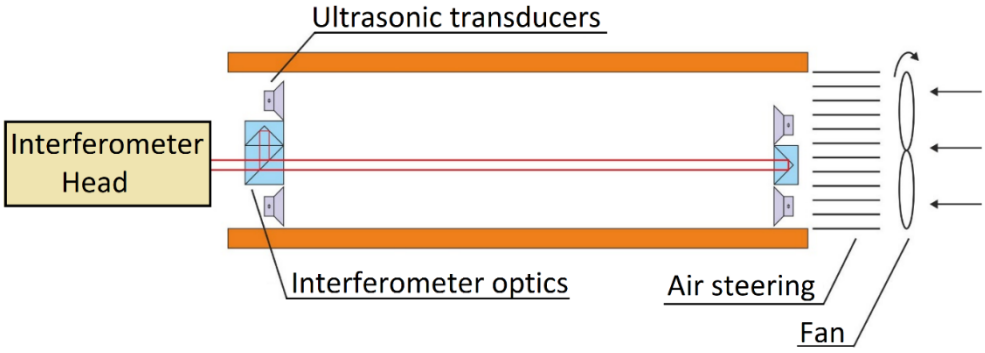

Figure 10. The set-up for testing the influence of air movement on the accuracy of temperature gradient compensation by the proposed ultrasonic technique.

has been compensated to the range of 0.1 μm. For the 32 min cycle of changes (figure 8(b)), fluctuations of the compensated course are not visible, and the readings have been compensated to 0.2 μm.

For longer cycles, from 60 min (figures 8(c) and (d)) the indications have been compensated to 0.2 μm, but other influences of temperature changes, e.g. the geometry of the mechanical elements of the system, are revealed. This may be due to the heat transfer between the chamber and the ground, and its expansion and deformation of the mechanical interferometer assemblies.

The impossibility of obtaining a better compensation of the temperature influence can also be caused by Abbe's error, due to the technical limitation of the axis mounting of the ultrasonic transmitter in the interference measurement axis, and thus the uneven spatial distribution of temperature at the location of both measurements. In addition, the influence on the uncertainty of compensation has the inertia of pressure and humidity sensors.

However, in all cases, a significant improvement in the stability of the interferometer indications is observed. It is evident that the applied measurement method allows us to improve the accuracy of the interferometric measurements, allowing significant compensation of changes in air temperature (especially short-term), taking into account its inhomogeneous spatial distribution.

3.3. Influence of air movement

The direction of air movement in relation to the measuring axis of the interferometer can be divided into two components, perpendicular and parallel to the measurement axis. Let us analyze both cases separately.

When the air flow with velocity υ is in the direction perpendicular to the direction of the measuring path the sound wavefront is shifted by a distance Δs, as shown in figure 9. This corresponds to the shift of the ultrasonic wave from the source S to the apparent source S'. The path the wave travels to the detection point D will change from Δl to $\Delta l'$.

Thus, the speed of the sound will be determined based on the duration of the sound travelling along $\Delta l'$. It will therefore be smaller than the correct one—determined on the basis of Δl. Based on the geometry of the drawing, we can write the equation

$$(v_{\mathrm{m}}t_{\mathrm{m}})^2 + (\upsilon t_{\mathrm{m}})^2 = (\nu t_{\mathrm{m}})^2 \tag{25}$$

where ν denotes the actual sound velocity, v_{m} represents the measured speed based on the distance $\Delta l'$, υ denotes the air velocity and t_{m} is the time measured on the distance $\Delta l'$. From here we will get an erroneously measured speed of sound in the form:

$$v_{\mathrm{m}} = \sqrt{\nu^2 - \upsilon^2}\,. \tag{26}$$

For the measurement length equal to $\Delta l = 1$ m, the sound speed υ correctly measured is equal to 335 m s^{-1} (the value adopted for theoretical considerations). At air velocity, e.g. $\upsilon = 1$ m s^{-1}, the measured velocity v_{m} is equal to 334.9985 m s^{-1}. Such an error in determining the speed of sound corresponds to a change in the ambient temperature by 0.004 °C. The sound velocity is determined by the arithmetic mean of two measurements; therefore, the resulting error caused by the transverse air movement will take the value of 0.008 °C. So, under typical conditions, it can be assumed that the transverse air movement with a velocity not exceeding 1 m s^{-1} can usually be neglected.

If the sound wave propagates in the direction consistent with or opposite to the direction of air movement, the wave's speed increases or decreases, respectively, by the value of the air velocity [15]. Using two tracks, in which the propagation of the sound wave takes place in the opposite directions, with the air moving parallel to the tracks, in one of them there will be an increase in the speed of sound propagation, and in the second a decrease by the same value. The arithmetic mean of the wave velocity determined in this way should not be changed. Below, we present the results of the tests verifying the effectiveness of the aforementioned compensation of air flow.

A previously described tunnel isolating the system from outside environmental conditions was used for the tests (figure 10). The air flow was forced by a fan.

To obtain a laminar flow of air, the fan was equipped with a jet guide consisting of many thin tubes. Due to the short measurement time (about 5 min) and high heat capacity of the bench it can be assumed that during the tests there were

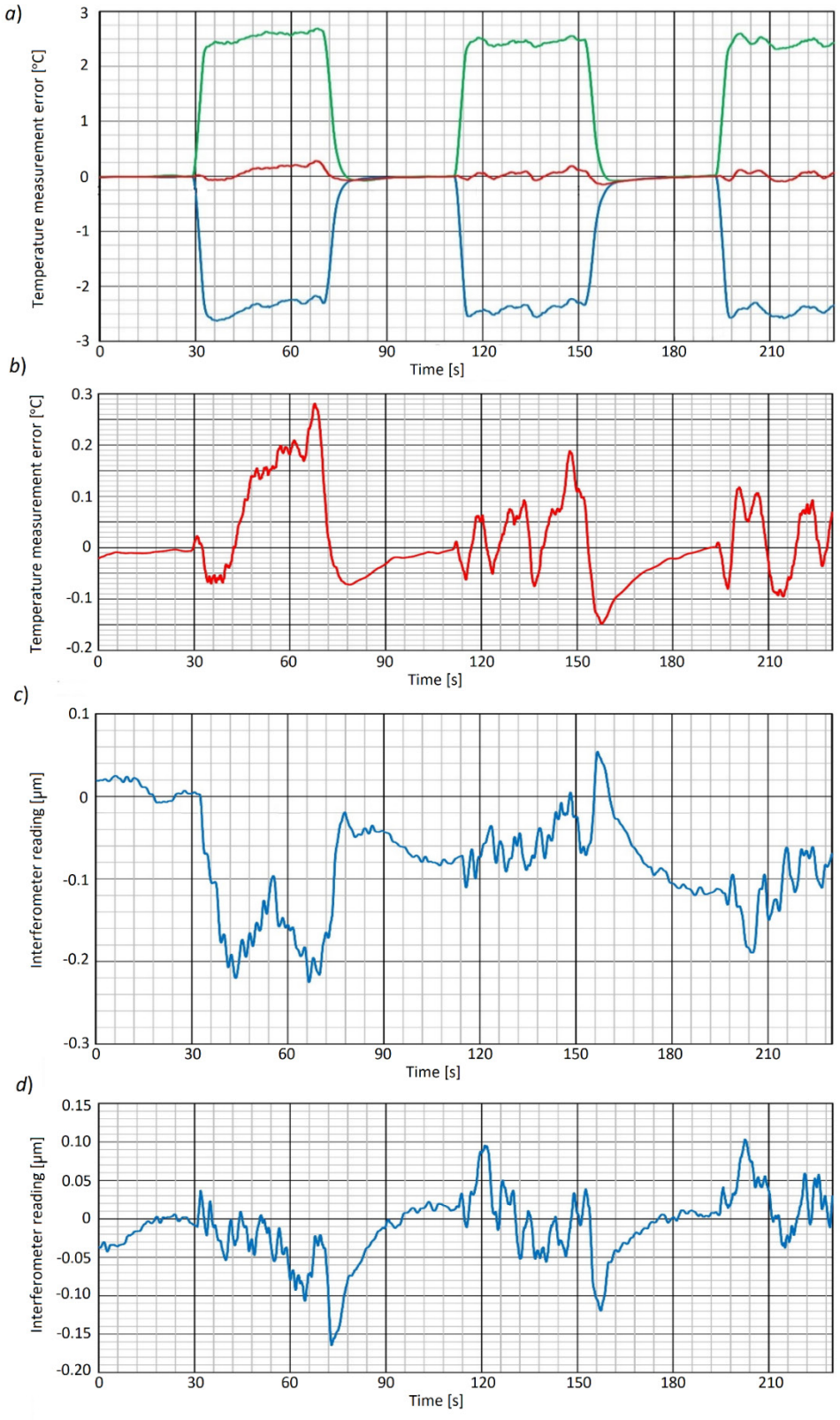

Figure 11. Exemplary results of the research on the influence of air flow along the measurement axis in the presented ultrasonic measurement. (a) Indications of ultrasound tracks. (b) The average of the indications of both tracks. (c) Indication of the interferometer without compensation. (d) Compensated indications of the interferometer.

no changes in the length of the measuring section. Also, it was possible to assume negligible changes in pressure and air humidity during the measurement. The length of the measured distance was approximately 1 m. During the measurement, changes in the readings of the interferometer and ultrasonic system were recorded. One measurement series consisted of four cycles of switching on and off airflow lasting about 80 s each. During the cycle, 40 s of fan operation followed and 40 s of break. The air flow rate was equal to approx. 1 m s^{-1}. All the registered changes have been calculated to obtain the temperature errors generated by air movement. The sample results are illustrated in figure 11. The graphs show changes in the readings of the interferometer and ultrasound system in relation to the first reading.

Changes in temperature indications determined in the ultrasound path caused by air movement are illustrated by the graph in figure 11(a). The upper and lower lines show changes in the readings in both ultrasound tracks operating in opposite directions. During air flow through the measuring tunnel, a single detector recorded changes in the speed of sound, which, calculated as a thermal correction, would correspond to 2.5 °C. This error should be compensated by applying a differential measurement from both tracks. The middle line represents the average indications of both tracks. Enlarged deviations in the mean value from zero are shown in figure 11(b). It can be seen that the temperature measurement error reaches 0.3 °C in the first cycle and decreases to 0.15 °C in the third cycle. The obtained results suggest that during the experiments the air temperature in the laboratory could slightly differ from the temperature in the tunnel. The indications had stabilized only after the fan was turned on and the air was replaced. Confirmation of the different temperature in the tunnel and outside it is the raw result of the interferometer (figure 11(c))—the difference in its readings reaches 0.25 μm. Another source of errors in the interference measurement, with the occurrence of air movement, is changes in atmospheric pressure caused by the air flow. In addition, the changes in the refractive index generated this way caused the deflection of the laser beam, and as a result, changed the optical path. However, after compensation in the entire series of measurements, the interferometer readings do not differ from the initial ones by more than 0.15 ° C, as shown in figure 11(d).

Summarizing the obtained exemplary results shows` that even with a very strong air flow (about 1 m s^{-1}) and with the turbulence associated with it, it is possible to reduce the temperature measurement error in the proposed ultrasonic system at least tenfold.

4. Conclusions

One of the main problems in intermediate length measurements waiting for an effective solution is minimization of the measurement error caused by the influence of ambient temperature variation along the measuring path. One of the methods to take into account the temporal and spatial temperature variability is the ultrasonic method of temperature measurement. The introduction of the paper presents an overview of the currently used ultrasonic temperature measurement methods, indicating that the bidirectional measurement technique with two ultrasound tracks potentially gives the best metrological and functional parameters. An article has been devoted to new proposals for the realization of this technique.

At the beginning of the theoretical part of the article, a method for determining the air temperature along the axis of the laser beam using the ultrasonic technique was proposed. The question is: what is the difference between the refractive index determined along the measurement path by ultrasound and the purely theoretically determined coefficient using the commonly used Edlén's equation using hypothetically infinitely many temperature sensors reproducing the distribution of its variability? Due to the complexity of Edlén's formula, its direct use to answer this question was not possible. To solve this problem, the authors proposed replacing the Edlén equation, by an approximate equation in the form of an appropriate second-degree polynomial. An important part of the analysis was the selection of polynomial coefficients so as to minimize the difference between the refractive index determined using the Edlén's formula and by the proposed approximate relationship. The regression coefficients obtained by the bisection method gave a satisfactory approximation error equal to approx. $3 \cdot 10^{-9}$, which in most cases may be omitted.

Based on this approximation we calculated the difference between the refractive index determined along the measurement path using the Edlén equation and by the ultrasound technique. For this analysis we assumed the value of the maximum temperature gradient that can appear along the measurement path to be equal to 0.1 °C/10 mm. For this value in the most unfavorable case, the error of approximation of the refractive index using the ultrasonic method was equal to about 30 ppb along the 1 m measuring path. This way, it was theoretically proved that the ultrasound method correctly takes into account the unknown temperature distribution along the measurement path.

To enable ultrasonic temperature measurement when the measuring reflector is moving, an iterative measurement algorithm has been proposed. The essence of the proposed algorithm is the lack of requirement to use point temperature sensors.

Experimental tests of the method were carried out in the system in which two ultrasonic paths parallel to the laser beam operated at different frequencies and continuous waves were emitted in opposite directions. At the beginning of the experimental verification the accuracy of the ultrasonic temperature measurements that it was possible to obtain was assessed. In the performed test, changes in the ambient temperature of about 1 °C generated the interferometric measurement error after temperature compensation based on the ultrasonic method over the length of 1 m in the range not exceeding ±0.03 μm. This range corresponds to a temperature change of approx. ±0.03 °C. Note that the obtained temperature measurement error also takes into account the impact of pressure and humidity gradients that may have occurred along the optical path. This inaccuracy is similar to that obtained with the spot thermometer. However, this inaccuracy concerns the value determined for the entire length of the measurement path, in real time.

An important property of ultrasonic measurement is that it allows one to improve the accuracy of interferometric measurements, allowing significant compensation of changes in air temperature (especially short-term), taking into account its inhomogeneous spatial distribution. The performed tests have shown that the variability in the results of the interference measurements resulting from thermal gradients has been compensated to the level of 0.1 μm along 1 m measuring distance.

The principle of the applied ultrasonic technique results is that it is sensitive to air flow. This influence was analyzed theoretically and experimentally. Theoretically, it was shown that the transverse (to the measuring direction) air flow with a velocity not exceeding 1 m s^{-1} can be neglected.

If the sound wave propagates in the direction consistent with or opposite to the direction of air movement, the wave's speed increases or decreases, respectively, by the value of the air velocity. The average value of the ultrasonic wave velocities calculated from measurements performed in two measuring tracks, in which the propagation of the sound wave takes place in the opposite directions, should be independent of air flow. Experimental verification has shown that even with a very strong air flow (about 1 m s^{-1}) and with the turbulence associated with it, it is possible to reduce the temperature measurement error in the proposed ultrasonic system at least tenfold.

In conclusion, the article shows that the proposed measurement technique can significantly improve the accuracy of interferometric displacement measurements in conditions that diverge from laboratory environments, i.e. when the temperature distribution is not constant along the measurement path and there is also air flow.

Acknowledgments

This work was supported by statutory funds (institution: Institute of Metrology and Biomedical Engineering, Warsaw University of Technology).

ORCID iDs

Marek Dobosz https://orcid.org/0000-0001-9062-1473

References

[1] Huang K N 2002 High precision, fast ultrasonic thermometer based on measurement of the speed of sound in air *Rev. Sci. Instrum.* **73** 4022–7
[2] Astrua M *et al* 2014 Air temperature measurements based on the speed of sound to compensate long distance interferometric measurements *EPJ Web of Conf.* **77** 00013
[3] Ezerioha N 2009 Ultrasonic thermometry in the verification of accurate displacement measurements in laser interferometry *Program Report* 1-23 SIST
[4] Korpelainen V and Lassila A 2004 Acoustic method for determination of the effective temperature and refractive index of air in accurate length interferometry *Opt. Eng.* **43** 2400–9
[5] Korpelainen V and Lassila A 2004 Online determination of the refractive index of air by ultrasonic speed of sound measurement for interferometric displacement measurements, ODIMAP IV pp 72–7
[6] Budzyń G and Rzepka J 2011 Method for the measurement of linear and angular displacements as well as the interferometer for measuring linear and angular displacements *Polish Patent* No. PL207983
[7] West D 1997 Acoustic thermometer *US Patent* No. US5624188A
[8] Jia R *et al* 2016 Study of ultrasonic thermometry based on ultrasonic time-of-flight measurement *AIP Adv.* **6** 035006
[9] Hayashi Y *et al* 1994 Ultrasonic temperature measuring apparatus *US Patent* No. US5360268
[10] Huang K N *et al* 2003 Temperature measurement system based on ultrasonic phase-shift method *IEEE EMBS Asian-Pacific Conf. on Biomedical Engineering (Kyoto, Japan, 20–22 October 2003)* pp 294–5
[11] Huang Y S *et al* 2007 An accurate air temperature measurement system based on an envelope pulsed ultrasonic time-of-flight technique *Rev. Sci. Instrum.* **78** 115102
[12] Tsai W *et al* 2006 High accuracy ultrasonic air temperature measurement using multi-frequency continuous wave *Sens. Actuators* A **132** 526–32
[13] Barshan B 2000 Fast processing techniques for accurate ultrasonic range measurements *Meas. Sci. Technol.* **11** 45–50
[14] Angrisani L *et al* 2006 A measurement method based on Kalman filtering for ultrasonic time-of-flight estimation *IEEE Trans. Instrum. Meas.* **55** 442–8
[15] Obraz J 1983 *Ultradźwięki w technice pomiarowej*, WNT (in Polish)
[16] Ebrahimkhanlou A and Salamone S 2017 A single-sensor approach based on multimodal edge reflections *Ultrasonics* **78** 134–45
[17] Ebrahimkhanlou A and Salamone S 2017 A probabilistic framework for single-sensor acoustic emission source localization in thin metallic plates *Smart Mater. Struct.* **26** 095026
[18] Huang Y P *et al* 2007 Envelope pulsed ultrasonic distance measurement system based upon amplitude modulation and phase modulation *Rev. Sci. Instrum.* **78** 065103
[19] Srinivasan K *et al* 2013 Acoustic pyrometry in flames Measurement **46** 315–323
[20] Huang K and Huang Y 2009 Multiple-frequency ultrasonic distance measurement using direct digital frequency synthesizers *Sens. Actuators* A **149** 42–50
[21] Zuckerwar A J 2002 *Handbook of the Speed of Sound in Real Gases* (San Diego, CA: Elsevier)
[22] Hallewell G D and Lynnworth L C 1994 A simplified formula for the analysis of binary gas containing a low concentration of a heavy vapor in a lighter carrier *Proc. of IEEE Ultrasonics Symp.* vol 3, pp 1311–6
[23] Cadet C, Valdes J L and Mitchell J W 1994 Ultrasonic time-of-flight method for on-line quantitation of semiconductor gases *Proc. of IEEE Ultrasonics Symp.* vol 3, pp 295–300
[24] Halliday D, Resnick R and Walker J 2013 *Fundamentals of Physics* 10th edn (New York: Wiley)
[25] Engineering ToolBox 2003 Specific heat and individual gas constant of gases The National Institute of Standards and Technology (NIST) (www.engineeringtoolbox.com/specific-heat-capacity-gases-d_159.html) (Accessed: October 2019)
[26] Monteith J L and Unsworth M H 2013 *Principles of Environmental Physics* 4th edn (New York: Academic)
[27] ISO 13788:2012-12 *Hygrothermal performance of building components and building elements — Internal surface temperature to avoid critical surface humidity and interstitial condensation — Calculation methods* (International Organization for Standardization)

[28] Born M and Wolf E 1999 *Principles of Optics* 7th edn (Cambridge: Cambridge University Press)
[29] Birch K P and Downs M J 1994 Correction to the updated Edlén equation for the refractive index of air *Metrologia* **31** 315–6
[30] Stone J A and Zimmerman J H 2003 Index of refraction of air, vacuum wavelength and ambient conditions based on modified Edlén equation, ENGINEERING METROLOGY TOOLBOX 2019 The National Institute of Standards and Technology (NIST) (http://emtoolbox.nist.gov/Wavelength/Edlen.asp) (Accessed: October 2019)
[31] Stone J A and Zimmerman J H 2001 Index of Refraction of Air National Institute of Standards and Technology (https://emtoolbox.nist.gov/Wavelength/Documentation.asp) (Accessed: October 2019)
[32] Ciddor E 1996 Refractive index of air: new equations for the visible and near infrared *Appl. Opt.* **35** 1566–73
[33] Stone J A and Zimmerman J H 2003 Index of refraction of air, vacuum wavelength and ambient conditions based on Ciddor equation, ENGINEERING METROLOGY TOOLBOX 2019 The National Institute of Standards and Technology (NIST) (http://emtoolbox.nist.gov/Wavelength/Ciddor.asp) (Accessed: October 2019)
[34] Ściuba M 2018 Ultrasound compensation of the influence of air temperature on interference length measurement *PhD Dissertation* Warsaw University of Technology
[35] Godin O A *et al* 2014 Passive acoustic measurements of wind velocity and sound speed in air *J. Acoust. Soc. Am.* **135** EL68–74